Research Article | Vol. 25, No. 23 | 13 Nov 2017 | OPTICS EXPRESS 28459
Optics EXPRESS

Complete dispersion characterization of microstructured optical fibers from a single interferogram using the windowed Fourier-ridges algorithm

TÍMEA GRÓSZ,* MERCÉDESZ HORVÁTH, AND ATTILA P. KOVÁCS

Department of Optics and Quantum Electronics, University of Szeged, Dóm tér 9, H-6720 Szeged, Hungary
**tgrosz@physx.u-szeged.hu*

Abstract: If multiple pulses, either higher-order or polarization modes, simultaneously travel in a fiber, they might overlap in the time domain, hindering dispersion retrieval of the modes in question using conventional evaluation techniques. In this work, a high-resolution windowed Fourier-ridges (WFR) algorithm is developed for evaluation of spectrally resolved interferograms produced by light pulses that are overlapping in time. The sufficiency of one spectral interferogram to retrieve the differential group dispersion and the polarization dependent chromatic dispersion directly with high accuracy is demonstrated on a meter-long HC-800-02 photonic crystal fiber. Results are in accordance with previously published data.

OCIS codes: (060.2300) Fiber measurements; (060.5295) Photonic crystal fibers; (120.3180) Interferometry; (260.1440) Birefringence; (260.2030) Dispersion.

References and links

1. J. Broeng, S. E. Barkou, T. Søndergaard, and A. Bjarklev, "Analysis of air-guiding photonic bandgap fibers," Opt. Lett. **25**(2), 96–98 (2000).
2. G. Bouwmans, F. Luan, J. Knight, P. St J Russell, L. Farr, B. Mangan, and H. Sabert, "Properties of a hollow-core photonic bandgap fiber at 850 nm wavelength," Opt. Express **11**(14), 1613–1620 (2003).
3. W. Göbel, A. Nimmerjahn, and F. Helmchen, "Distortion-free delivery of nanojoule femtosecond pulses from a Ti:sapphire laser through a hollow-core photonic crystal fiber," Opt. Lett. **29**(11), 1285–1287 (2004).
4. A. A. Ishaaya, C. J. Hensley, B. Shim, S. Schrauth, K. W. Koch, and A. L. Gaeta, "Highly-efficient coupling of linearly- and radially-polarized femtosecond pulses in hollow-core photonic band-gap fibers," Opt. Express **17**(21), 18630–18637 (2009).
5. T. Grósz, A. P. Kovács, and K. Varjú, "Chromatic Dispersion Measurement along Both Polarization Directions of a Birefringent Hollow-core Photonic Crystal Fiber Using Spectral Interferometry," Appl. Opt. **56**(19), 5369–5376 (2017).
6. M. A. Galle, W. S. Mohammed, L. Qian, and P. W. E. Smith, "Single-arm three-wave interferometer for measuring dispersion of short lengths of fiber," Opt. Express **15**(25), 16896–16908 (2007).
7. T. Grósz, A. P. Kovács, M. Kiss, and R. Szipőcs, "Measurement of higher order chromatic dispersion in a photonic bandgap fiber: comparative study of spectral interferometric methods," Appl. Opt. **53**(9), 1929–1937 (2014).
8. Q. Kemao, "Windowed Fourier transform for fringe pattern analysis," Appl. Opt. **43**(13), 2695–2702 (2004).
9. Q. Kemao, "On window size selection in the windowed Fourier ridges algorithm," Opt. Lasers Eng. **45**, 1186–1192 (2007).
10. Q. Kemao, "Applications of windowed Fourier fringe analysis in optical measurement: A review," Opt. Lasers Eng. **66**, 67–73 (2015).
11. L. Huang, Q. Kemao, B. Pan, and A. K. Asundi, "Comparison of Fourier transform, windowed Fourier transform, and wavelet transform methods for phase extraction from a single fringe pattern in fringe projection profilometry," Opt. Lasers Eng. **48**, 141–148 (2010).
12. S. K. Debnath, M. P. Kothiyal, and S.-W. Kim, "Evaluation of spectral phase in spectrally resolved white-light interferometry: Comparative study of single-frame techniques," Opt. Lasers Eng. **47**, 1125–1130 (2009).
13. P. Hlubina, J. Lunacek, D. Ciprian, and R. Chlebus, "Windowed Fourier transform applied in the wavelength domain to process the spectral interference signals," Opt. Commun. **281**, 2349–2354 (2008).
14. P. Hlubina and D. Ciprian, "Absolute phase birefringence dispersion in polarization-maintaining fiber or birefringent crystal retrieved from a channeled spectrum," Opt. Lett. **35**(10), 1566–1568 (2010).

#303815 https://doi.org/10.1364/OE.25.028459
Journal © 2017 Received 17 Aug 2017; revised 23 Sep 2017; accepted 28 Sep 2017; published 2 Nov 2017

Optics EXPRESS

15. J. W. Nicholson, L. Meng, J. M. Fini, R. S. Windeler, A. DeSantolo, E. Monberg, F. DiMarcello, Y. Dulashko, M. Hassan, and R. Ortiz, "Measuring higher-order modes in a low-loss, hollow-core, photonic-bandgap fiber," Opt. Express **20**(18), 20494–20505 (2012).
16. X. Chen, M. J. Li, N. Venkataraman, M. Gallagher, W. Wood, A. Crowley, J. Carberry, L. Zenteno, and K. Koch, "Highly birefringent hollow-core photonic bandgap fiber," Opt. Express **12**(16), 3888–3893 (2004).
17. M. Takeda, H. Ina, and S. Kobayashi, "Fourier-transform method of fringe-pattern analysis for computer-based topography and interferometry," J. Opt. Soc. Am. **72**(1), 156–160 (1982).
18. D. K. Gifford, B. J. Soller, M. S. Wolfe, and M. E. Froggatt, "Optical vector network analyzer for single-scan measurements of loss, group delay, and polarization mode dispersion," Appl. Opt. **44**(34), 7282–7286 (2005).
19. J. Bethge, C. Grebing, and G. Steinmeyer, "A fast Gabor wavelet transform for high-precision phase retrieval in spectral interferometry," Opt. Express **15**(22), 14313–14321 (2007).
20. http://www.nktphotonics.com/wp-content/uploads/sites/3/2015/01/HC-800.pdf.
21. T. Grósz, A. P. Kovács, K. Mecseki, L. Gulyás, and R. Szipőcs, "Monitoring the dominance of higher-order chromatic dispersion with spectral interferometry using the stationary phase point method," Opt. Commun. **338**, 292–299 (2015).

1. Introduction

With the invention and fabrication of hollow-core photonic crystal fibers (HC-PCFs) [1–4] numerous applications requiring low-loss pulse delivery with special dispersion characteristics became available. Since the PCF structure can be modified almost arbitrarily, theoretically, the requirements of any specific application can be met with proper design. Nevertheless, no matter how advance the manufacturing process becomes, small variations between the desired and the realized geometry and therefore in the optical properties still remain. As most applications are sensitive to noise introduced by interfering coherent modes, detecting the presence of higher-order modes is beneficial. Furthermore, since in birefringent fibers polarization mode dispersion can be an issue, determining the differential group dispersion (DGD), i.e., the delay between the orthogonally propagating modes is of great interest. Considering that the dispersion properties of the polarization directions can be quite distinct [2,5], and therefore the effect on the pulse having parallel polarization with the fast or slow direction is also different [5], determining the dispersion along both axes is also of vital importance.

Spectrally resolved interferometry is a well-proven, extremely sensitive linear method suitable for the chromatic dispersion measurement of fibers as well [6]. Different methods [7] can be used to evaluate the recorded interferograms one of which is the windowed Fourier-transform (WFT) method primarily used in profilometry [8–12]. Over the years two approaches have been developed for signal processing based on the WFT [8,10,11]. The first approach filters the fringe pattern in the windowed Fourier domain (windowed Fourier-filtering, WFF) [12–14], while the second approach uses a ridge-based algorithm (windowed Fourier-ridges, WFR) [9]. The importance and effects in connection with the window size were discussed in details using simulations [9]. The WFF was found suitable for the retrieval of the dispersion of beam splitters [10,13] and the DGD in polarization-maintaining fibers [14]. Nicholson *et al.* used a similar technique called sliding-window FT to examine the wavelength dependence of the mode structure in a HC-PCF operating at 1550 nm [15], however, the WFT was basically a visualization tool, and no quantitative dispersion retrieval was done based on it. A low-resolution WFR method was used to retrieve the group beat length and group birefringence in highly birefringent HC-PCFs [16]. The WFR technique was also employed in the dispersion retrieval of a specially designed Bragg fiber, however, since the spectral resolution had to be increased to resolve the resonances appearing in the group delay curve of the fiber, the WFT signal was broadened hindering precise ridge tracking [7]. The Fourier-transform (FT) method [17,18], on the other hand, was found to be a high-precision evaluation technique even for higher-order dispersion [5,7]. Its accuracy is remarkable especially if the fiber under test exhibits sharp resonances in its spectrum, like the Bragg fiber mentioned above [7]. Evaluations based on the wavelet transform using ridge tracking and search for center of gravity have also been employed in the spectral phase retrieval [19]. The performance of the WFT and the wavelet transform was investigated with

Optics EXPRESS

simulations [8,9] and experiments [11-12] as well, which revealed that the wavelet transform is not necessarily good for fringe pattern analysis, since it provides the results with more noise compared to the WFT.

In the case of birefringent fibers, it is rather hard to ensure that only one polarization mode is excited. Similarly, in multimode fibers one cannot guarantee that only the fundamental mode is guided. If multiple pulses, either polarization or higher-order modes, travel in the fiber, they might overlap in the time domain, which raises difficulties during filtering even for the FT method [18]. Provided that the spectrum of the tested fiber sample is free from resonances, a high-resolution WFR method might be able to overcome this obstacle.

In this work a WFR algorithm with high spectral resolution is used to evaluate the chromatic dispersion of a HC-800-02 PCF (NKT Photonics) [5,20] along both polarization directions while obtaining DGD information as well. We demonstrate that the WFR algorithm is suitable for evaluation of spectrally resolved interferograms obtained in the case of two sample pulses overlapping in time. It is shown that recording one interferogram is sufficient to retrieve the dispersion curves for the two polarization directions and the DGD curve directly with high accuracy. Results are in accordance with previously published data [5], corroborating the applicability of the WFR method even in cases where no attention is paid to the excitation of only one polarization direction.

2. Theory

In spectrally resolved interferometry a combination of a two-beam interferometer, a broadband light source and a spectrometer is used. The optical sample under study is placed in one arm of the interferometer while the other is used as a reference and produces adjustable delay. At given τ time delays between the arms spectral interference fringes appear at the output of the spectrometer. The frequency-dependent intensity distribution of the fringes *I(ω)* can be written as

$$I(\omega) = I_r(\omega) + I_s(\omega) + 2\sqrt{I_r(\omega)I_s(\omega)}\cos(\Phi(\omega)), \tag{1}$$

where $I_r(\omega)$ and $I_s(\omega)$ describe the spectral intensity distributions of the reference and the sample beams respectively, and $\Phi(\omega)$ stands for the spectral phase difference between the two arms:

$$\Phi(\omega) = \varphi(\omega) + \omega\tau, \tag{2}$$

where $\varphi(\omega)$ denotes the spectral phase of the sample, and $\omega\tau$ is the phase induced by the path length difference between the two arms. In most cases the spectral phase is used to describe the changes in the temporal intensity profile of an ultrashort laser pulse as a result of propagation in a dispersive optical medium. The coefficients of the Taylor expansion of $\varphi(\omega)$ can be used to characterize the spectral phase,

$$\varphi(\omega) \approx \varphi(\omega_0) + \left.\frac{d\varphi}{d\omega}\right|_{\omega=\omega_0}(\omega-\omega_0) + \frac{1}{2}\left.\frac{d^2\varphi}{d\omega^2}\right|_{\omega=\omega_0}(\omega-\omega_0)^2 + \frac{1}{6}\left.\frac{d^3\varphi}{d\omega^3}\right|_{\omega=\omega_0}(\omega-\omega_0)^3 + \ldots, \tag{3}$$

where ω_0 denotes the carrier frequency of the pulse. The derivatives of the spectral phase with respect to the angular frequency evaluated at ω_0 are called the constant phase term ($\varphi(\omega_0)$), the group delay (GD), the group-delay dispersion (GDD) and the third-order dispersion (TOD), respectively, as follows:

$$GD(\omega_0) = \left.\frac{d\varphi}{d\omega}\right|_{\omega=\omega_0}, GDD(\omega_0) = \left.\frac{d^2\varphi}{d\omega^2}\right|_{\omega=\omega_0}, TOD(\omega_0) = \left.\frac{d^3\varphi}{d\omega^3}\right|_{\omega=\omega_0}. \tag{4}$$

Optics EXPRESS

Using these coefficients, the GDD(ω) function and the dispersion parameter D of the sample can be calculated,

$$GDD(\omega) = GDD(\omega_0) + TOD(\omega_0)(\omega - \omega_0) + ..., \tag{5}$$

$$D(\omega) = -\frac{GDD(\omega) \cdot 2\pi c}{\lambda^2 L}, \tag{6}$$

where λ is the wavelength, c is the velocity of light in vacuum, and L denotes the length of the fiber. Please note that the GDD is proportional to the length of the fiber while D is normalized to the length.

Once the spectral interferogram is recorded, the spectral phase and thus the dispersion can be retrieved in several ways [7,12]. The evaluation method considered here is based on the windowed Fourier-ridges algorithm [9,10]. First, an inverse Fourier-transform is performed on the interferogram given by Eq. (1) that is multiplied by a window function:

$$W_I(\Omega, t) = \int_{-\infty}^{\infty} I(\omega) g(\omega - \Omega) \exp(i\omega t) d\omega, \tag{7}$$

where

$$g(\omega - \Omega) = \exp\left[-\left(\frac{\omega - \Omega}{\Delta\Omega} \right)^2 \right] \tag{8}$$

is a Gaussian window function, Ω is the central frequency and $\Delta\Omega$ is the width of the window function. As Ω is changed, a series of the windowed interferograms are obtained. Introducing $a(\omega) = I_s(\omega) + I_r(\omega)$ and $b(\omega) = 2\sqrt{I_s(\omega) I_r(\omega)}$, and substituting the cosine function in Eq. (1) with the corresponding complex exponential function we get

$$I(\omega) = a(\omega) + \frac{b(\omega)}{2} \exp(i\Phi(\omega)) + \frac{b(\omega)}{2} \exp(-i\Phi(\omega)). \tag{9}$$

Note that since $a(\omega)$ in Eq. (9) is a slowly varying function of ω its inverse Fourier-transform appears around $t = 0$. On the other hand, $b(\omega)$, which contains the important information on the dispersion of the sample, changes rapidly with ω and its inverse Fourier-transform results in two symmetrical signals around $\tau + GD(\omega_0)$ and $-\tau - GD(\omega_0)$. Considering the one appearing at $\tau + GD(\omega_0)$ from Eq. (7) we get

$$W_f(\Omega, t) = \int_{-\infty}^{\infty} \frac{b(\omega)}{2} g(\omega - \Omega) \exp\left[i\omega t - i\Phi(\omega) \right] d\omega. \tag{10}$$

The width $\Delta\Omega$ of the window function should be set to fulfil the following two conditions: in the vicinity of Ω the fringe amplitude is constant, i.e., $b(\omega) = b(\Omega)$ and a linear approximation can be used for the spectral phase, i.e.,

$$\Phi(\omega) = \Phi(\Omega) + \left. \frac{d\Phi}{d\omega} \right|_{\Omega} (\omega - \Omega). \tag{11}$$

From Eqs. (2) and (4) we get

$$\frac{d\Phi}{d\omega} = GD(\omega) + \tau. \tag{12}$$

By introducing

Optics EXPRESS

$$\begin{aligned}\xi &= \omega - \Omega \\ d\xi &= d\omega\end{aligned} \tag{13}$$

from Eq. (10) we get

$$W_f(\Omega,t) = \frac{b(\Omega)}{2}\exp\left[-i(\Phi(\Omega)-\Omega t)\right]\int_{-\infty}^{\infty} g(\xi)\exp\left[(i(t-\Phi'(\Omega))\xi)d\xi\right] \tag{14}$$

where $\Phi'(\Omega)$ denotes the first derivative of the spectral phase with respect to the angular frequency ω evaluated at Ω. Rewriting Eq. (14)

$$W_f(\Omega,t) = \frac{b(\Omega)}{2}\exp\left[-i(\Phi(\Omega)-\Omega t)\right]G\left[(t-\Phi'(\Omega))\right], \tag{15}$$

we obtain a signal with a Gaussian envelope, where the ridge of the envelope is given by

$$t_p(\Omega) = \Phi'(\Omega). \tag{16}$$

Using Eqs. (12) and (16) we get

$$GD(\Omega) = t_p(\Omega) - \tau. \tag{17}$$

By determining the ridges of the WFT signal, t_p at each Ω frequency the relative GD curve of the sample can be obtained. If the time delay τ is changed, the relative GD curve moves along the time axis as well, but since its shape does not change, the relative GD of the sample can be determined by fitting a polynomial to the ridges. Differentiating Eq. (17) the GDD of the sample can also be retrieved

$$GDD(\Omega) = \frac{dt_p}{d\Omega}. \tag{18}$$

Using Eq. (6) the dispersion parameter of the sample can be evaluated:

$$D(\Omega) = -\frac{2\pi c}{\lambda^2 L}\frac{dt_p}{d\Omega}. \tag{19}$$

Although D is not dependent on the time delay τ, selecting the proper delay is of crucial importance since it is proportional to the fringe density and therefore affects their visibility.

Consider the case when two pulses having orthogonal polarization directions propagate in the sample arm. Equation (1) is modified as

$$\begin{aligned}I(\omega) = I_r(\omega) + I_{sx}(\omega) + I_{sy}(\omega) + 2\sqrt{I_r(\omega)I_{sx}(\omega)}\cos(\Phi_x(\omega)) + \\ +2\sqrt{I_r(\omega)I_{sy}(\omega)}\cos(\Phi_y(\omega)) + 2\sqrt{I_{sx}(\omega)I_{sy}(\omega)}\cos(\Phi_{xy}(\omega)),\end{aligned} \tag{20}$$

where $I_{sx} = I_{sx0}\cos^2\alpha$ and $I_{sy} = I_{sy0}\sin^2\alpha$ are the projections of intensities of the sample pulses onto the plane of the polarization of the reference pulse. α denotes the angle between the polarization plane *x-z* of the sample pulse and the polarization plane of the reference pulse. I_{sx0} and I_{sy0} are the intensities of the sample pulses polarized linearly in the *x-z* and *y-z* planes, respectively. The first two interference terms describe the interference of the reference pulse and the sample pulse propagating along the fast (x) and the slow (y) axes, respectively, and the last term expresses the interference between the sample pulses. The corresponding spectral phases can be written as

Optics EXPRESS

$$\begin{aligned}\Phi_x(\omega) &= \varphi_x(\omega) + \omega\tau,\\ \Phi_y(\omega) &= \varphi_y(\omega) + \omega\tau,\\ \Phi_{xy}(\omega) &= \varphi_x(\omega) - \varphi_y(\omega).\end{aligned} \tag{21}$$

Now the $W_f(\Omega, t)$ is composed of three terms, therefore three t_p ridges can be defined:

$$\begin{aligned}t_{px}(\Omega) &= \Phi'_x(\Omega),\\ t_{py}(\Omega) &= \Phi'_y(\Omega),\\ t_{pxy}(\Omega) &= \Phi'_{xy}(\Omega).\end{aligned} \tag{22}$$

Note, that the interference of the two sample pulses with each other and the reference pulse, results in three GD curves:

$$\begin{aligned}GD_x(\Omega) &= t_{px}(\Omega) - \tau,\\ GD_y(\Omega) &= t_{py}(\Omega) - \tau,\\ DGD(\Omega) &= t_{pxy}(\Omega).\end{aligned} \tag{23}$$

3. Experimental

The experimental setup shown in Fig. 1 comprised a Mach-Zehnder interferometer illuminated by an ultrabroadband Ti:Sapphire oscillator (Femtolasers, Rainbow, 6 fs@800 nm, FWHM = 150 nm) and a high-resolution spectrometer (Ocean Optics, HR4000, 700 to 900 nm, spectral resolution 0.2 nm). The fiber under test was a 97.5-cm-long hollow-core PCF (HC-800-02, NKT Photonics) [20], identical to the one tested in a previous work [5]. A polarizer before the setup was used to ensure the purity of linear polarization. A half-wave plate was placed in the sample arm before the fiber to facilitate the excitation of one or both polarization modes of the fiber simultaneously. A half-wave plate was placed in the reference arm as well to produce beams with matching polarization. Near-IR achromatic lenses of 30 mm and 19 mm focal lengths served as coupling and collimating optics, respectively. Since identical lenses were placed in the reference arm, their dispersion was compensated. A polarizer at the output of the interferometer was used to optimize the visibility of the fringes and to facilitate the interference of orthogonally polarized beams if set to 45° with respect to the interfering polarization directions.

After the spectrally resolved interferogram is obtained at the output of the spectrometer it can be evaluated in several ways. In the case of the WFR method the use of Gaussian window functions with varying central frequencies [blue-dashed curve in Fig. 1] results in a similar signal as shown below.

Optics EXPRESS

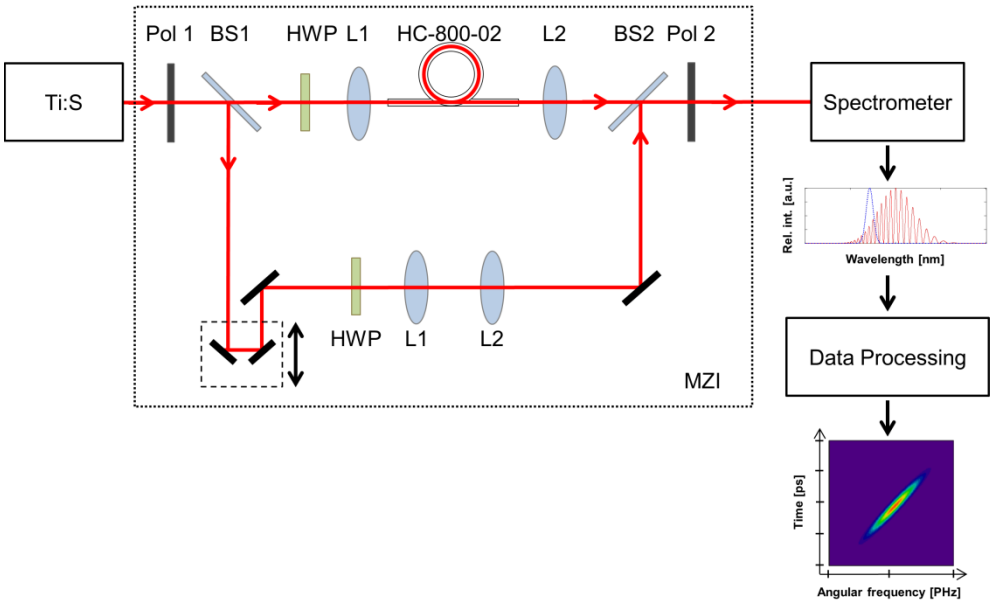

Fig. 1. Scheme of the experimental setup with a simulated spectrally resolved interferogram and a WFT signal obtained after processing this interferogram. Ti:S: Ti:Sapphire oscillator, MZI: Mach-Zehnder interferometer, Pol1 and Pol2: first and second linear polarizer, BS1 and BS2: first and second beam splitter, HWP: half-wave plate, and L1 and L2: coupling and collimating lenses.

4. Results and discussion

As established earlier, although the HC-800-02 fiber is single-mode, it supports two orthogonally polarized modes. If both are excited, either accidentally or intentionally, they may interfere with each other and also with the reference beam, provided it has a matching polarization component. Recording and evaluating such an interferogram may provide information on the chromatic dispersion properties of both polarization modes and the DGD as well.

To test this hypothesis the half-wave plate in the sample arm was set to excite both polarization modes of the fiber equally, and the polarizer at the output and the half-wave plate in the reference arm were set also at 45° with respect to the polarization directions of the fiber [2,14,15]. The resulting interferogram is shown in Fig. 2(a). First, it was processed with the conventional FT method. Having taken the inverse FT we can see three signals [Fig. 2(b)]: the first appearing at approximately 1 ps belongs to the DGD, the second and the third around 9 and 10 ps can be assigned to the interference of the pulse traveling in the fast and the slow axis of the fiber with the reference pulse, respectively. Note that here only the amplitudes of these complex signals are shown. The spectral phase is usually obtained by performing a FT on the complex signal of interest which is filtered first [blue-dashed curve in Fig. 2(b)]. As can be seen, in this case the last two signals overlap in time, which hinders filtering the correct signal and the dispersion retrieval along a given direction [18]. If we filter these signals together anyway and perform a FT, the spectral phase can only be obtained [Fig. 2(c)] with a large error. This is corroborated by the large misfit seen between the retrieved and the fitted curves regardless of the order of the fitted polynomial [Fig. 2(d)].

Optics EXPRESS

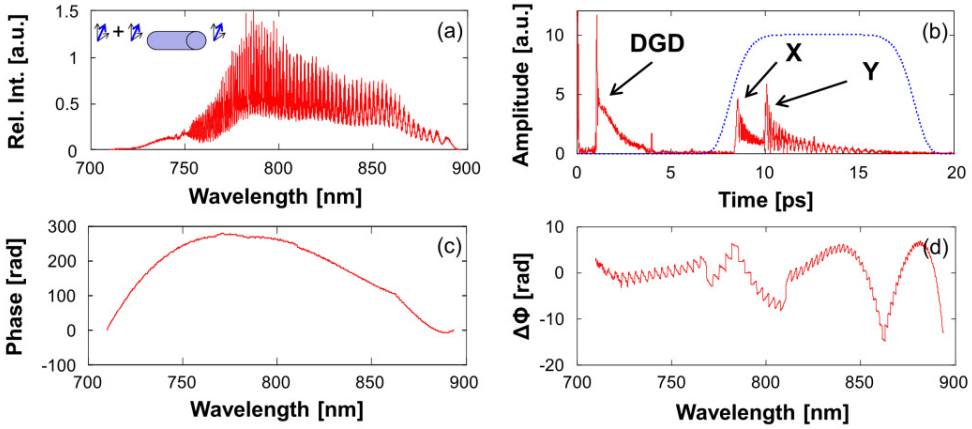

Fig. 2. (a) The recorded interferogram, (b) its Fourier-transform, (c) the retrieved spectral phase without the linear phase term, and (d) the difference between the measured and fitted phase curve when both polarization modes are excited simultaneously with the reference beam.

Exactly the same interferogram was also evaluated using the WFR method. The width of the window function was carefully set to be small enough to fulfill the criteria stated in Section 2 and Eq. (11), but large enough to avoid spectral narrowing, which would broaden the WFT signal in time. In order to minimize the time broadening and the peak-shifting effect caused by the GDD and TOD, respectively, we set the width of the window function to limit the time broadening to 10%. That was achieved by choosing a window function having a width of 5 THz. The spectral resolution was 4 THz, therefore the window functions slightly overlapped. Since the time delay between the arms of the interferometer is unchanged, the WFT signals corresponding to the interfering sample pulses and the reference pulses also appear around 9 and 10 ps, however, in this case they can be distinguished [Figs. 3(a) and 3(b)] while with the conventional FT method they cannot. After obtaining the WFT signals the center of gravity of the three signals was determined over the spectral range of 2.1 and 2.5 PHz. In the following step a polynomial of the desired order, in our case a fifth order polynomial, was fitted to these data, and the actual GD curves were acquired [blue curves in Fig. 3(a)].

As can be seen, by determining the ridges of the aforementioned three signals in principle, a single recorded interferogram is sufficient to retrieve the relative GD curves and thus the dispersion properties of both polarization modes along with the DGD curve at the same time. To test the precision of this approach, the WFR method was also applied on interferograms recorded while only one polarization direction was excited that interfered with the reference beam [Figs. 3(c) and 3(d)]. Note that these WFT signals appeared at different time positions contrary to the case when both polarization modes were excited simultaneously. That is simply because they were recorded at different time delays between the arms of the interferometer. About 20 interferograms were evaluated for the fast and the slow directions in total. Additionally, the PMD was measured while exciting both polarization modes equally and blocking the reference arm [Fig. 3(e)].

Optics EXPRESS

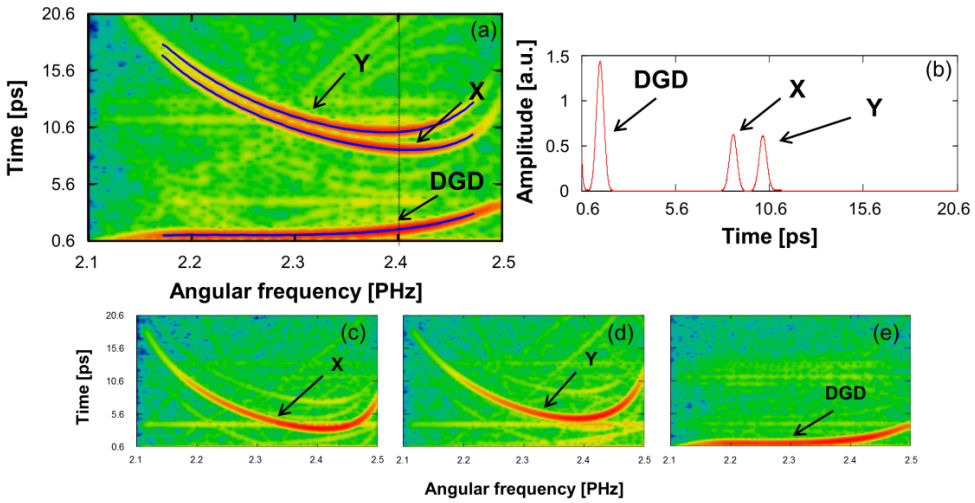

Fig. 3. (a) Windowed Fourier-transform of the recorded interferogram and (b) amplitude profile along a selected frequency of 2.4 THz when both polarization modes are excited simultaneously and interfere with the reference beam. WFT signals when (c) the fast or (d) the slow mode individually interferes with the reference beam set at the same position in both cases, and (e) both polarization modes are excited without the reference beam.

In Fig. 4 the retrieved D curves for the fast and the slow axes and the DGD curves are shown in the case of simultaneous and separate excitation between 762 nm (2.47 PHz) and 867 nm (2.17 PHz). As can be seen the curves are completely identical regardless of the excitation conditions. Also, these results are in complete agreement with previously published results [5] obtained with the conventional FT method when the polarization modes were excited separately [Fig. 4 green-dotted curves]. Note that this observation confirms the sufficiency of a single interferogram for high-precision characterization of the polarization dependent chromatic dispersion and the DGD using the WFR algorithm in the case of the tested birefringent HC-PCF sample. Although the DGD curve can be determined by exciting the orthogonal polarization modes separately and subtracting their GD curves obtained at the same delay, it should be emphasized that its direct retrieval using our method is more precise, especially in the case of longer fiber samples [5]. Although the WFR method is slightly more time-consuming than the FT technique, the complete dispersion characterization from a single recorded interferogram makes it rather appealing. Furthermore, there is a possibility to predict the sign and the dominance of higher order dispersion visually from the shape of the ridges of the WFT signal without further signal processing. For instance, the convex shape of the ridges indicates the dominance of the positive TOD component. The fact that an asymmetry appears in the lower frequency domain suggests negative GDD [21]. These observations are also in complete agreement with previously published data [5].

Optics EXPRESS

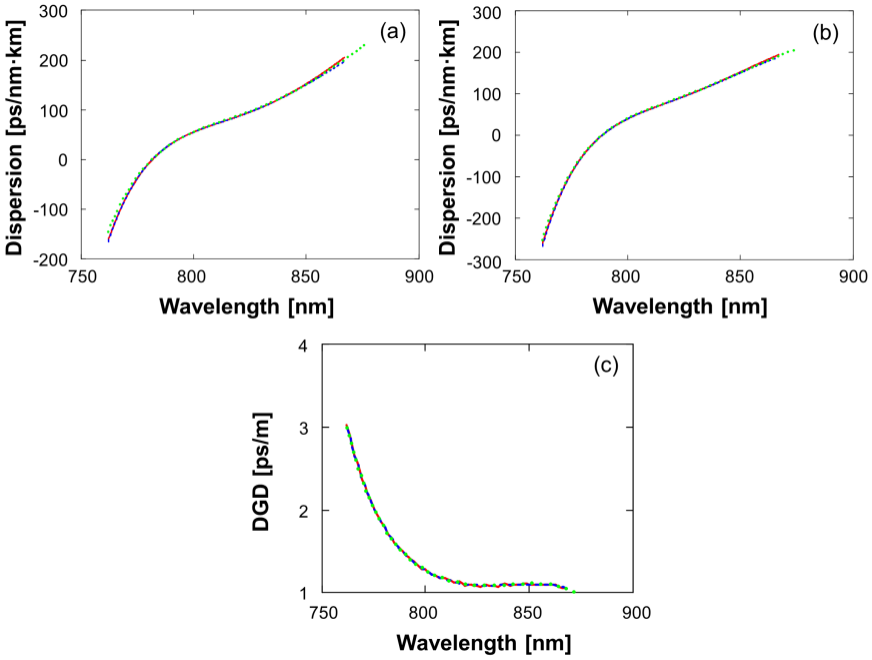

Fig. 4. Dispersion along (a) the fast and (b) the slow axes for a 97.5-cm-long sample determined during simultaneous (red curve) and separate excitation (blue-dashed curve) of the polarization modes. (c) Differential group delay curves referring to a 1-m-long fiber determined during simultaneous excitation of the polarization modes with (red curve) and without (blue-dashed curve) the reference beam. The results of the FT method during separate excitation of the polarization modes are also shown for comparison (green-dotted curve) [5].

5. Conclusions

The differential group dispersion and the polarization dependent chromatic dispersion of a HC-800-02 photonic crystal fiber were retrieved experimentally between 762 and 867 nm utilizing an ultrabroadband Ti:Sapphire oscillator, a Mach-Zehnder interferometer, and a high-resolution spectrometer. A WFR algorithm with high spectral resolution was developed to process spectrally resolved interferograms resulting in WFT signals that are very close to each other in the time domain.

It is shown, that the DGD and the chromatic dispersion along the two polarization directions can be determined directly with high accuracy using a single interferogram if we excite both orthogonal modes simultaneously and have them interfere with a reference beam. Another advantage of the method is that the sign and the dominance of higher order dispersion can also be predicted visually from the shape of the ridges of the WFT signal without further signal processing. All results are in accordance with previously published data [5], corroborating the applicability of the WFR method even in cases where no attention is paid to the excitation of only one polarization direction.